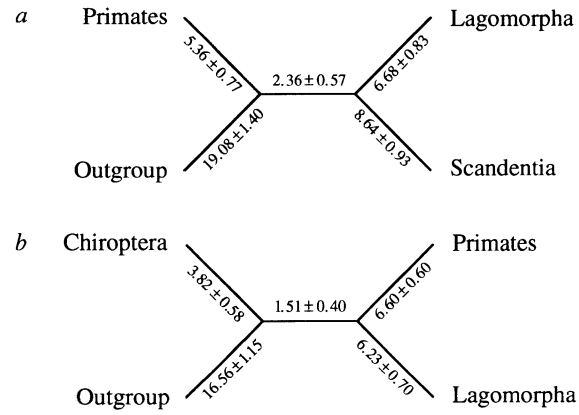

FIG. 2 Maximum-likelihood trees for Lagomorpha, Primates, an outgroup, and Scandentia (*a*) or Chiroptera (*b*). Maximum-likelihood branch lengths (±s.e.) are given in units of amino-acid replacements per 100 amino-acid sites. *a*, The tree is based on 7 orthogolous protein sequences (1,157 amino acids). *b*, This tree is based 9 proteins (1,433 amino acids).

strongly supported by analyses of complete mitochondrial DNA sequences (Ú. Árnason, personal communication). Therefore, cohort Anagalidia or the positioning of Macroscelidea as an immediate outgroup to a monophyletic Glires are invalidated by the molecular data. We can also reject the monophyly of Glires by noting that four taxa other than Primates, these being Artiodactyla + Cetacea, Carnivora, Scandentia, and Dermoptera, are significantly closer phylogenetically to Lagomorpha than are the rodents (data not shown).

Finally, we tried to pinpoint more accurately the phylogenetic position of Lagomorpha. Three orders are thought on morphological grounds to be closely related to the primates: Scandentia, Dermoptera and Chiroptera[6], which together are included within a superordinal taxon called Archonta. Scandentia is considered particularly close phylogenetically to Primates, and the two orders are joined in morphological systems of classification within a superorder called Primatomorpha, whereas Chiroptera and Dermoptera form a sister superordinal taxon called Volitantia[6]. In a maximum-likelihood analysis, Scandentia was found to cluster with Lagomorpha to the exclusion of Primates and the outgroup (Fig. 2*a*), with a log-likelihood bootstrap probability of 0.80, as opposed to 0.17 for the tree in which Primatomorpha is monophyletic. Primates clustered with Lagomorpha to the exclusion of Chiroptera, a phylogenetic arrangement supported by a log-likelihood bootstrap probability of 0.74, as opposed to 0.07 for the tree in which Archonta is monophyletic (Fig. 2*b*). These results add to the accumulating molecular evidence against the monophyly of Archonta[10]. The phylogenetic position of Dermoptera relative to Primates and Lagomorpha could not be resolved with the available data (3 proteins, 629 amino acids). Pending a significant increase in the database for dermopterans and scandentians, we conclude tentatively that Scandentia and Lagomorpha are sister orders.

About a dozen anatomical 'synapomorphies' form the morphological basis for the clustering of Rodentia and Lagomorpha[3]. Some of them, such as 'orbitosphenoid relatively large' or 'incisive foramina enlarged' are so vaguely defined as to defy objective analysis. Other traits, such as a 'blastocyst attachment invasive', also typify other eutherian orders, but these conditions are usually brushed aside as being 'derived secondarily'. Many character-state resemblances between rodents and lagomorphs, for example, the absence of canines, are related to specializations due to the evolution of gnawing in both orders, and as such may be subject to rampant parallelism[1]. Finally, the polarities of morphological character states as either 'derived' or 'primitive' are decided on the basis of comparisons with a eutherian 'morphotype', an artificial construct based on assumptions about hypothetical ancestral taxa. Errors in polarity identification may alter the phylogenetic tree considerably. Our molecular results indicate that a reassessment of the morphological evidence is needed. One simple and intriguing possible resolution of the conflict between morphological and molecular data is to assume that many morphological 'synapomorphies' used in support of Glires are actually ancestral character states that have been retained in some mammalian orders but were lost in others. If this reversal of character-state polarity proves valid, then the ancestral eutherian morphotype may have resembled a rodent species much more closely than is currently recognized in the morphopalaeontological literature. □

Received 24 July; accepted 17 November 1995.

1. Wood, A. E. *Evolution* **11,** 417–425 (1957).
2. Novacek, M. J., Wyss, A. R. & McKenna, M. C. in *Phylogeny of the Tetrapods* Vol. 2 (ed. Benton, M. J.) 31–71 (Oxford Univ. Press, 1988).
3. Luckett, W. P. & Hartenberger, J.-L. J. *Mamm. Evol.* **1,** 127–147 (1993).
4. Casane, D., Dennebouy, N., de Rochambeau, H., Mounolou, J. C. & Monnerot, M. *Genetics* **138,** 471–480 (1994).
5. Mignotte, F., Gueride, M., Champagne, A. M. & Mounolou, J. C. *Eur. J. Biochem.* **194,** 561–571 (1990).
6. Novacek, M. J. *Nature* **356,** 121–125 (1992).
7. McKenna, M. C. in *Phylogeny of the Primates* (eds Luckett, W. R. & Szalay, F. S.) 21–46 (Plenum, New York, 1975).
8. Miyamoto, M. M. & Goodman, M. *Syst. Zool.* **35,** 230–240 (1986).
9. Li, W.-H., Gouy, M., Sharp, P. A., O'hUigin, C. & Yang, Y.-W. *Proc. natn. Acad. Sci. U.S.A.* **87,** 6703–6707 (1990).
10. Bailey, W. J., Slightom, J. L. & Goodman, M. *Science* **256,** 86–89 (1992).
11. Easteal, S. *Genetics* **124,** 165–173 (1990).
12. de Jong, W. W., Leunissen, J. A. M. & Wistow, G. J. in *Mammalian Phylogeny: Placentals* (eds Szalay, F. S., Novacek, M. J. & McKenna, M. C.) 5–12 (Springer, New York, 1993).
13. Duret, L., Mouchiroud, D. & Gouy, M. *Nucleic Acids Res.* **22,** 2360–2365 (1994).
14. George, D. G., Barker, W. C., Mewes, H. W., Pfeiffer, F. & Tsugita, A. *Nucleic Acids Res.* **22,** 3569–3573 (1994).
15. Thompson, J. D., Higgins, D. G. & Gibson, T. J. *Nucleic Acids Res.* **22,** 4673–4780 (1994).
16. Graur, D., Hide, W. A. & Li, W.-H. *Nature* **351,** 649–652 (1991).
17. Graur, D., Hide, W. A., Zharkikh, A. & Li, W.-H. *Comp. Biochem. Physiol.* **101B,** 495–498 (1992).
18. Milinkovitch, M. C. *Trends Ecol. Evol.* **10,** 328–334 (1995).
19. Saitou, N. & Nei, M. *Molec. Biol. Evol.* **4,** 406–425 (1987).
20. Felsenstein, J. *Cladistics* **5,** 164–166 (1989).
21. Adachi, J. & Hasegawa, M. *MOLPHY: Programs for Molecular Phylogentics. I. PROTML; Maximum Likelihood Inference for Protein Phylogeny. Computer Science Monographys, no 27.* (Institute of Statistical Mathematics, Tokyo, 1992).
22. Kimura, M. *The Neutral Theory of Molecular Evolution* (Cambridge Univ. Press, 1983).
23. Felsenstein, J. *Evolution* **39,** 783–791 (1985).
24. Li, W.-H. *Molec. Biol. Evol.* **6,** 424–435 (1989).
25. Kishino, H., Miyata, T. & Hasegawa, M. *J. molec. Evol.* **30,** 151–160 (1990).

ACKNOWLEDGEMENTS. The initial data compilation was done under the auspices of the National Center for Biotechnological Information at the National Institutes of Health. Further collection of data and analyses were performed while D. G. was a recipient of an EMBO short-term fellowship. We thank Ú. Árnason for information on the mitochondrial DNA sequence of *Elephantulus*.

Molecular basis of sun-induced premature skin ageing and retinoid antagonism

Gary J. Fisher, Subhash C. Datta, Harvinder S. Talwar, Zeng-Quan Wang, James Varani*, Sewon Kang & John J. Voorhees

Departments of Dermatology and * Pathology, University of Michigan Medical School, Kresge 1, R6558, Ann Arbor, Michigan 48109–0528, USA

DAMAGE to skin collagen and elastin (extracellular matrix) is the hallmark of long-term exposure to solar ultraviolet irradiation[1–3], and is believed to be responsible for the wrinkled appearance of sun-exposed skin[4,5]. We report here that matrix-degrading metalloproteinase messenger RNAs, proteins and activities are induced in human skin *in vivo* within hours of exposure to ultraviolet-B irradiation (UVB). Induction of metalloproteinase proteins and activities occurred at UVB doses well below those that cause skin reddening. Within minutes, low-dose UVB

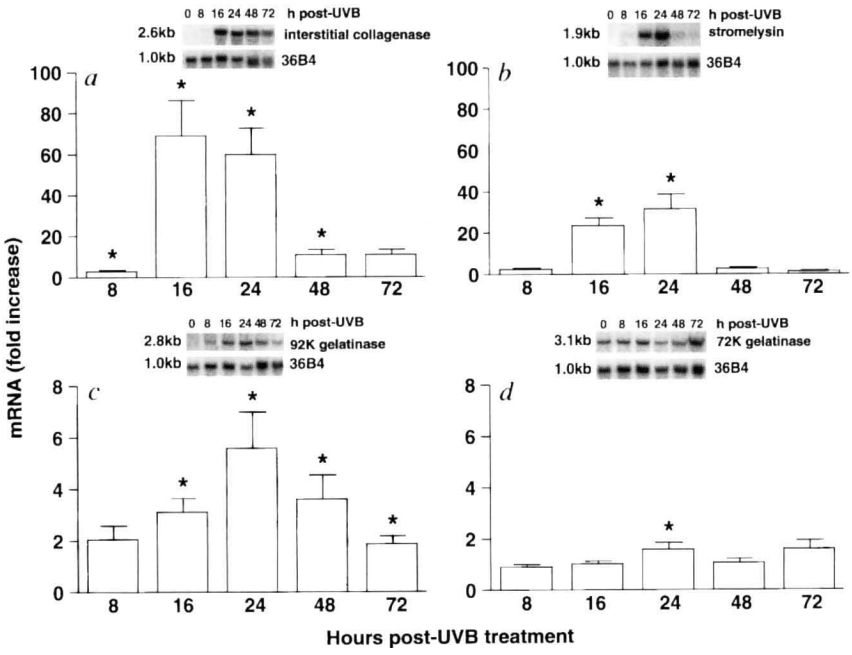

FIG. 1 UVB induces interstitial collagenase, 92K gelatinase, and stromelysin I mRNA, but not 72K gelatinase mRNA, in human skin *in vivo*. Adult buttocks were irradiated with 2 MED UVB. Irradiated sites and adjacent non-irradiated sites were removed at indicated times following irradiation. Tissue was snap-frozen, and total RNA isolated and analysed by northern blot[26]. Band intensities were quantitied using a PhosphorImager. Values for metalloproteinase transcripts were normalized to those for control gene *36B4*. Results are means ± s.e.m. ($n = 6$ for 8, 16, 48 and 72 h, and $n = 17$ for no-UVB control and 24 h), and are presented as fold increase of normalized values relative to non-irradiated skin. Insets show representative bands at indicated times after irradiation. *a*, Interstitial collagenase; *b*, stromelysin I; *c*, 92K gelatinase; *d*, 72K gelatinase. * $P < 0.05$ compared with no UVB control.

METHODS. Subjects were irradiated with an Ultralite Panelite lamp containing four F36T12 ERE-VHO UVB tubes. Irradiation intensity was monitored with an IL443 phototherapy radiometer and a SED240/UVB/W photodetector (International Light, Newbury, MA). UVB output, measured 48 cm from the source, was 0.5 mW cm^{-2}. Subjects were adult Caucasians (approximately equal numbers of males and females) with light to mild pigmentation. Minimal erythema dose (MED) UVB for each subject was determined 24 hours post irradiation. 1MED for all subjects ranged from 30–50 mJ cm^{-2}. For each subject, skin was removed by keratome[26] from four sites (one non-irradiated and three irradiated). Thus, bands displayed in figures are composites from several individuals. All subjects provided informed written consent, and procedures involving humans were approved by the University of Michigan Institutional Review Board. Northern analysis of UVB-treated skin with a stromelysin I-specific probe yielded results identical to those obtained with full length stromelysin I probe (*b*), whereas hybridization with a stromelysin II-specific probe yielded no signal. We conclude that UVB induces predominantly stromelysin I in human skin. Data were analysed by two-tailed paired *t*-test.

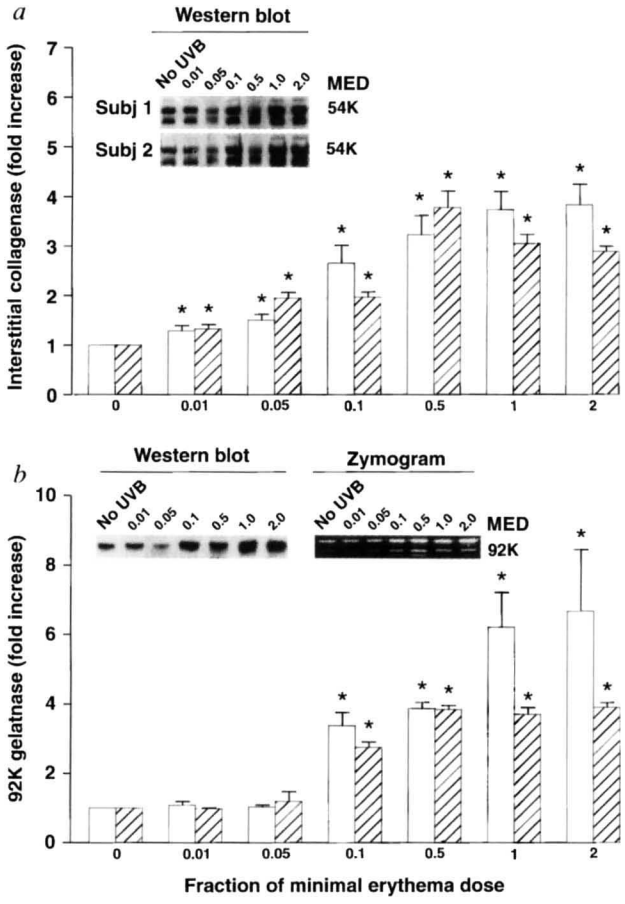

FIG. 2 Low-dose UVB induces interstitial collagenase and 92K gelatinase proteins and activities in human skin *in vivo*. Adult subjects were exposed to the indicated doses of UVB as described in Fig. 1 legend. Full thickness skin (6 mm cylinders) was obtained 24 hours after irradiation. *a*, Interstitial collagenase protein (□), determined by western blot, and activity (▨). The inset shows representative western blots from two subjects. The larger 54K band is intact interstitial collagenase, and the smaller 45K band is the proteolytically processed activated form of the molecule[11]. Note both forms of interstitial collagenase are elevated following UVB irradiation. *b*, 92K gelatinase protein (□), determined by western blot, and activity (▨). The inset shows a representative western blot (left panel) and a representative zymogram (right panel). Multiple bands on the zymogram are proteolytically processed active forms of the enzyme, determined by immunoblot of the zymogram (data not shown). Note unprocessed and processed forms of 92K gelatinase are induced by UVB. Band intensities were quantified by laser densitometry. Results are means ± s.e.m., $n = 10$; * $P < 0.025$ vs no UVB control.

METHODS. Skin from irradiated and adjacent non-irradiated sites was homogenized in 20 mM Tris-HCl (pH 7.6), 5 mM $CaCl_2$, and centrifuged at 3,000*g* for 10 min. Supernatants were used to measure interstitial collagenase and 92K gelatinase proteins by western blot (100 μg per lane), using chemiluminscence detection, and activities by hydrolysis of [^{3}H]fibrillar collagen[27] (100 μg per assay) and gelatin zymography[28] (20 μg per assay), respectively. Antibodies against interstitial collagenase[29] and 92K gelatinase[30] have been described.

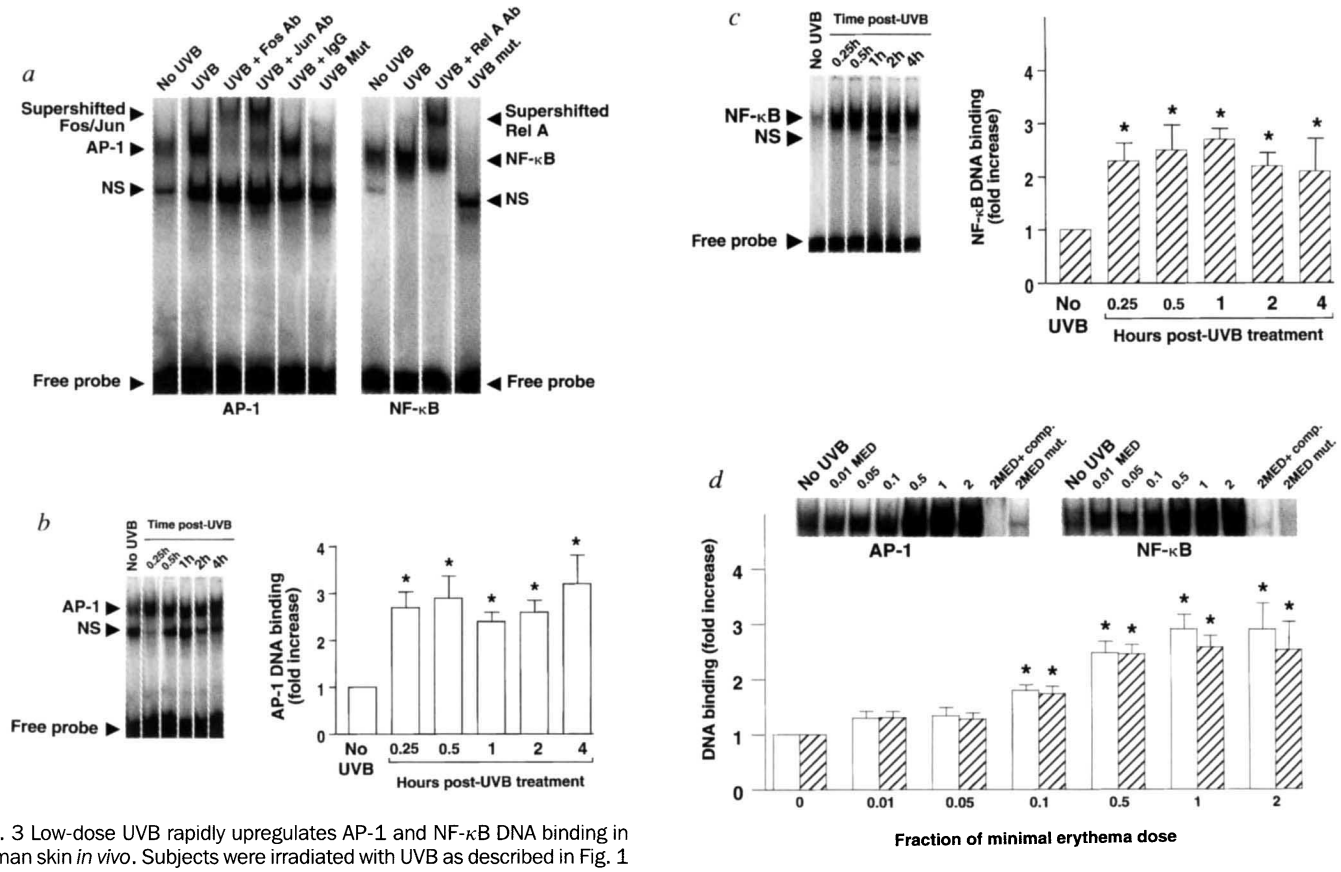

FIG. 3 Low-dose UVB rapidly upregulates AP-1 and NF-κB DNA binding in human skin *in vivo*. Subjects were irradiated with UVB as described in Fig. 1 legend. At the indicated times after irradiation, tissue was taken by keratome and immediately processed to obtain nuclear extracts. AP-1 and NF-κB binding to double-stranded DNA probes were measured by electrophoretic mobility-shift assays. *a*, AP-1 and NF-κB DNA binding in non-irradiated and irradiated (4 h after 2 MED UVB) skin. Supershifts using antibodies against Jun and Fos family members and p65/Rel A demonstrated the presence of these proteins in AP-1 and NF-κB retarded complexes, respectively. Reduced binding to mutant probes demonstrates specificity of AP-1 and NF-κB retarded complexes. NS, nonspecific complex. *b*, Time course of induction of AP-1 DNA binding by 2 MED UVB. Results are means ± s.e.m., $n = 9$. $^*P < 0.01$ compared with no UVB control. *c*, Time course of induction of NF-κB DNA binding by 2 MED UVB. Results are means ± s.e.m., $n = 9$. $^*P < 0.01$ compared with no UVB control. *d*, UVB dose-dependence of induction of AP-1 (white bars) and NF-κB (striped bars). DNA binding was measured 30 min after irradiation. $^*P < 0.02$ versus no UVB control. Also shown are representative AP-1 and NF-κB retarded complexes. +comp., Addition of 100-fold excess unlabelled probe. mut., Mutated ^{32}P-labelled probe. Intensities of retarded complexes were quantified by PhosphorImager. Results are means ± s.e.m., $n = 9$.

METHODS. Nuclear extracts were prepared from skin biopsies as described[21]. Biopsies (~200 mg wet weight) containing 10^8 cells yielded 500 μg nuclear extract protein, on average. Electrophoretic mobility-shift assays (8 μg nuclear extract protein) were performed using ^{32}P-labelled DNA probes containing AP-1 and NF-κB consensus and mutated DNA-binding sequences, as described[21]. SP-1 DNA binding was also determined, and found to not vary significantly between non-irradiated and irradiated samples (data not shown). Antibodies for supershifts were obtained from Santa Cruz Biotechnology. Jun and Fos antibodies had broad reactivity to all Jun and Fos family members, respectively. NF-κB antibody was specific for p65/Rel A.

upregulated the transcription factors AP-1 and NF-κB, which are known to be stimulators of metalloproteinase genes[6,7]. All-*trans* retinoic acid, which transrepresses AP-1 (ref. 8), applied before irradiation with UVB, substantially reduced AP-1 and metalloproteinase induction. We propose that elevated metalloproteinases, resulting from activation of AP-1 and NF-κB by low-dose solar irradiation, degrade collagen and elastin in skin. Such damage, if imperfectly repaired, would result in solar scars, which through accumulation from a lifetime of repeated low-dose sunlight exposure could cause premature skin ageing (photoageing).

We determined the time course of changes in interstitial collagenase, stromelysin I, gelatinase of relative molecular mass 92,000 (M_r 92K), and 72K gelatinase mRNA levels, following UVB exposure. These four metalloproteinases together possess the capacity to degrade collagenous and non-collagenous molecules in extracellular matrix of skin[9–12]. Human subjects were irradiated on buttock skin with twice the UVB dose required to cause barely perceptible skin reddening (minimal erythema dose, MED). Induction of interstitial collagenase (Fig. 1*a*), stromelysin I (Fig. 1*b*), and 92K gelatinase (Fig. 1*c*) mRNAs was maximal (6–60-fold) within 16 to 24 hours, and returned to near baseline within 48 to 72 hours. 72K gelatinase mRNA was detectable but was only elevated 1.6-fold at 24 hours post-UVB (Fig. 1*d*).

Time courses for induction of interstitial collagenase and 92K gelatinase proteins and activities by 2 MED UVB paralleled those observed for their mRNAs (data not shown). Also consistent with northern analysis, neither 72K gelatinase protein nor enzyme activity was induced (data not shown), and thus served as an internal control. Induction of interstitial collagenase (Fig. 2*a*) and 92K gelatinase (Fig. 2*b*) proteins and activities by UVB was dose-dependent, and for both metalloproteinases, changes in protein content and enzyme activity mirrored each other. Interstitial collagenase was induced by all doses of UVB tested (0.01–2 MED), whereas 92K gelatinase was induced by ⩾0.1 MED. Induction of both interstitial collagenase and 92K gelatinase was maximal at 1 MED and approximately half-maximal at 0.1 MED. This dose of UVB is equivalent to 2–3 min solar irradiation on a summer day, which causes no perceptible skin reddening. Skin injuries such as blisters and wounds induce interstitial collagenase, 92K gelatinase, and stromelysin in cells within or adjacent to extracellular matrix, where their substrates are localized[9,10]. It is likely therefore that metalloproteinases induced

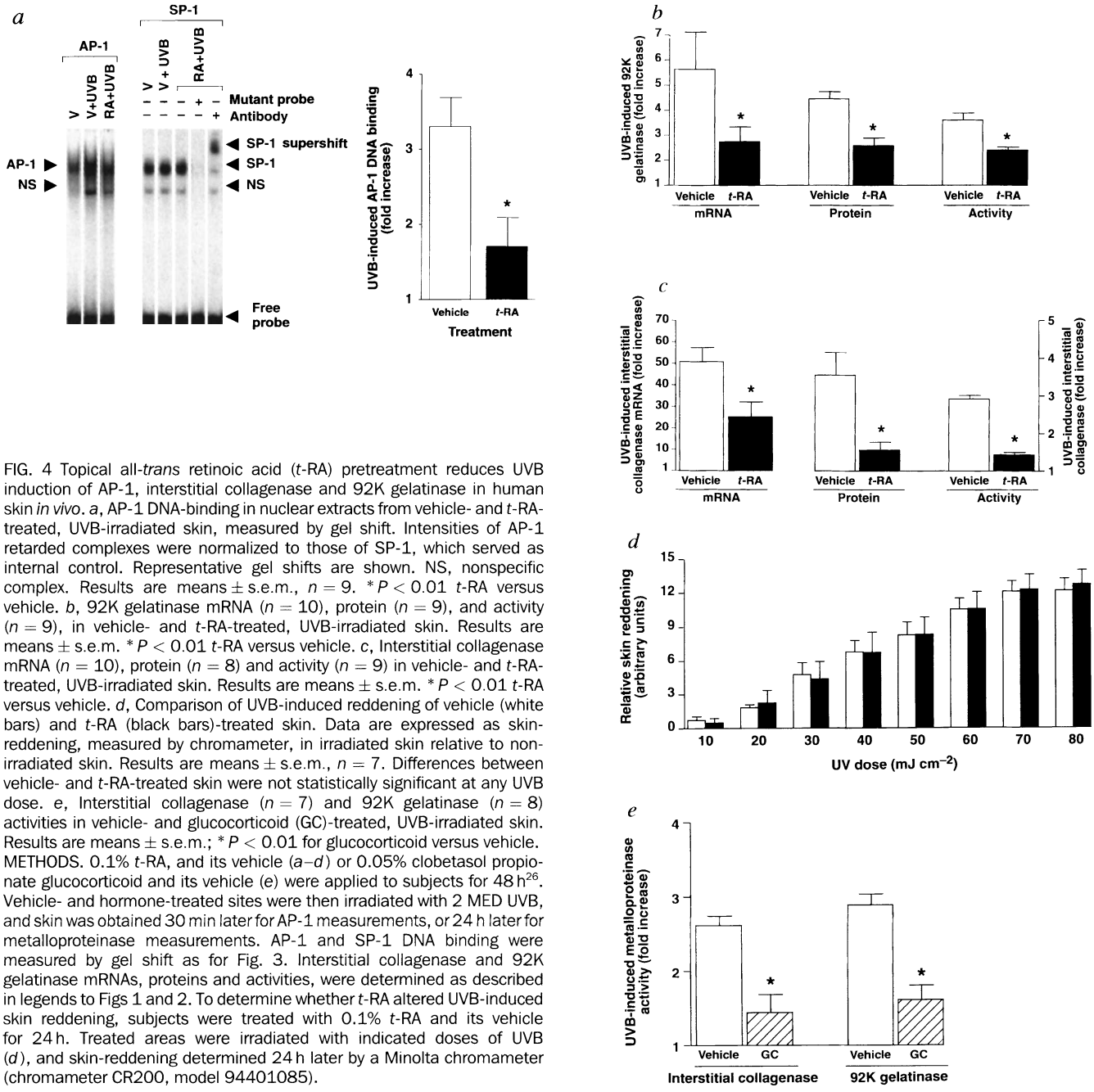

FIG. 4 Topical all-*trans* retinoic acid (*t*-RA) pretreatment reduces UVB induction of AP-1, interstitial collagenase and 92K gelatinase in human skin *in vivo*. *a*, AP-1 DNA-binding in nuclear extracts from vehicle- and *t*-RA-treated, UVB-irradiated skin, measured by gel shift. Intensities of AP-1 retarded complexes were normalized to those of SP-1, which served as internal control. Representative gel shifts are shown. NS, nonspecific complex. Results are means ± s.e.m., $n = 9$. * $P < 0.01$ *t*-RA versus vehicle. *b*, 92K gelatinase mRNA ($n = 10$), protein ($n = 9$), and activity ($n = 9$), in vehicle- and *t*-RA-treated, UVB-irradiated skin. Results are means ± s.e.m. * $P < 0.01$ *t*-RA versus vehicle. *c*, Interstitial collagenase mRNA ($n = 10$), protein ($n = 8$) and activity ($n = 9$) in vehicle- and *t*-RA-treated, UVB-irradiated skin. Results are means ± s.e.m. * $P < 0.01$ *t*-RA versus vehicle. *d*, Comparison of UVB-induced reddening of vehicle (white bars) and *t*-RA (black bars)-treated skin. Data are expressed as skin-reddening, measured by chromameter, in irradiated skin relative to non-irradiated skin. Results are means ± s.e.m., $n = 7$. Differences between vehicle- and *t*-RA-treated skin were not statistically significant at any UVB dose. *e*, Interstitial collagenase ($n = 7$) and 92K gelatinase ($n = 8$) activities in vehicle- and glucocorticoid (GC)-treated, UVB-irradiated skin. Results are means ± s.e.m.; * $P < 0.01$ for glucocorticoid versus vehicle. METHODS. 0.1% *t*-RA, and its vehicle (*a*–*d*) or 0.05% clobetasol propionate glucocorticoid and its vehicle (*e*) were applied to subjects for 48 h[26]. Vehicle- and hormone-treated sites were then irradiated with 2 MED UVB, and skin was obtained 30 min later for AP-1 measurements, or 24 h later for metalloproteinase measurements. AP-1 and SP-1 DNA binding were measured by gel shift as for Fig. 3. Interstitial collagenase and 92K gelatinase mRNAs, proteins and activities, were determined as described in legends to Figs 1 and 2. To determine whether *t*-RA altered UVB-induced skin reddening, subjects were treated with 0.1% *t*-RA and its vehicle for 24 h. Treated areas were irradiated with indicated doses of UVB (*d*), and skin-reddening determined 24 h later by a Minolta chromameter (chromameter CR200, model 94401085).

by UVB are localized to act on their extracellular matrix substrates, as occurs with other types of skin injury.

Transcription factors AP-1, composed of Jun and Fos proteins, and NF-κB, composed of Rel family members, are activated by a variety of extracellular stimuli, including short-wavelength UV (UVC)[13]. *In vitro*, stimulation of interstitial collagenase[14], 92K gelatinase[7], and stromelysin I (ref. 15) gene transcription by extracellular mediators is dependent upon activation and binding of AP-1 to specific sequences in their promoters. 92K-gelatinase gene transcription is also positively regulated by NF-κB (ref. 7). We therefore determined whether UVB irradiation regulates AP-1 and NF-κB in human skin *in vivo*.

Two MED UVB upregulated AP1-1 and NF-κB DNA binding (Fig. 3*a*). Binding of both transcription factors to their DNA response elements was specific, as demonstrated by loss of retarded complexes with mutated labelled probes (Fig. 3*a*). Antibody supershifts demonstrated that the specific AP-1 and NF-κB retarded complexes observed with extracts from UVB-irradiated skin contained Jun and Fos proteins, and Rel A protein, respectively (Fig. 3*a*). Induction of AP-1 (Fig. 3*b*) and NF-κB (Fig. 3*c*) by 2 MED UVB occurred within 15 min and remained elevated for at least 24 hours (data not shown). In contrast DNA binding of transcription factor SP-1, as an internal control, did not vary significantly between non-irradiated and irradiated samples at any time (data not shown).

Half-maximal induction of AP-1 and NF-κB, measured 30 min after irradiation, occurred at ~0.1 MED and maximal induction at 1 MED (Fig. 3*d*). The UVB dose dependencies for induction of AP-1 and NF-κB closely matched those observed for induction of interstitial collagenase and 92K gelatinase (Fig. 2), consistent with participation of AP-1 and NF-κB in UVB-induced increases in these metalloproteinases. Of note is that the 72K gelatinase gene is not induced by UVB, and does not contain either AP-1 or NF-κB response elements in its promoter[16].

Several members of the nuclear receptor superfamily, including retinoic acid[8,17] and glucocorticoid[18,19] receptors, are capable of

transrepressing AP-1 activity. Transrepression is ligand-dependent, and apparently involves protein–protein interactions between hormone receptors and Jun or Fos[20]. These interactions result in complexes that lack transactivation capacity for either AP-1 or hormone-response elements[20]. Pretreatment of skin, which expresses retinoic acid receptors[21], with all-*trans* retinoic acid (*t*-RA) reduced UVB-induced AP-1 DNA binding by 70% (Fig. 4*a*). *t*-RA pretreatment also reduced UVB-induced 92K gelatinase (Fig. 4*b*) and interstitial collagenase (Fig. 4*c*) mRNAs, proteins and activities by 50–80%. 72K gelatinase mRNA, protein and activity, which were not induced by UVB, were also not altered by *t*-RA (data not shown). Although *t*-RA absorption overlaps the UVB range (*t*-RA, λ_{max} 351 nm), *t*-RA did not reduce UVB-induced skin reddening (Fig. 4*d*) (that is, *t*-RA is not a sunscreen, at least for the chromophore(s) responsible for skin reddening), indicating that observed reductions in AP-1, interstitial collagenase and 92K gelatinase induction were specific, rather than being due to absorption of UVB by *t*-RA. Furthermore, glucocorticoid (λ_{max} 237 nm) pretreatment, which like *t*-RA has AP-1 transrepression activity, also reduced UVB-induced interstitial collagenase and 92K gelatinase activities to extents similar to *t*-RA (Fig. 4*e*). Our data are consistent with *t*-RA transrepression of AP-1-mediated induction of interstitial collagenase and 92K gelatinase, although limitations of *in vivo* experimentation mean that other mechanisms cannot be excluded.

Collagen and elastin provide structural integrity to skin[22]. Induction by sunlight of metalloproteases that degrade collagen and elastin in skin[12,23] may therefore be the primary mechanism mediating cutaneous photoageing. Based on our data, it is conceivable that *t*-RA, which improves photoageing once it has occurred[24], and other molecules that inhibit UVB-induced metalloproteinases[25], may reduce sun-induced collagen degradation and prevent photoageing in human skin. □

Received 31 July; accepted 24 November 1995.

1. Talwar, H. S., Griffiths, C. E. M., Fisher, G. J., Hamilton, T. A. & Voorhees, J. J. *J invest. Dermat.* **105,** 285–290 (1995).
2. Lavker, R. M. *J. invest. Dermat.* **73,** 559–566 (1979).
3. Smith, J. G., Davidson, E. A., Sams, W. M. & Clark, R. D. *J. invest. Dermat.* **39,** 347–350 (1962).
4. Kligman, L. H. & Kligman, A. M. *Photodermatology* **3,** 215–227 (1986).
5. Wlaschek, M. *et al. Photchem. Photobiol.* **59,** 550–556 (1994).
6. Angel, P. *et al. Cell* **49,** 729–739 (1987).
7. Sato, H. & Seiki, M. *Oncogene* **8,** 395–405 (1993).
8. Salbert, G. *et al. Molec. Endocr.* **7,** 1347–1356 (1993).
9. Oikarinen, A., Kylmaniemi, M., Autio-Harmainen, A., Autio, P. & Salo, T. *J. invest. Dermat.* **101,** 205–210 (1993).
10. Saarialho-Kere, U. K., Pentland, A. P., Birkedal-Hansen, H., Parks, W. C. & Welgus, H. G. *J. clin. Invest.* **94,** 79–88 (1994).
11. Mauch, C., Krieg, T. & Bauer, E. A. *Arch. Dermat. Res.* **287,** 107–114 (1994).
12. Eisen, A. Z. *J. Invest. Dermat.* **52,** 442–448 (1969).
13. Devary, Y., Gottlieb, R. A., Lau, L. F. & Karin, M. *Molec. cell. Biol.* **11,** 2804–2811 (1991).
14. Angel, P. & Karin, M. *Matrix Suppl.* **1,** 156–164 (1992).
15. Quinones, S., Buttice, G. & Kurkinen, M. *Biochem. J.* **302,** 471–477 (1994).
16. Frisch, S. M. & Morisaki, J. H. *Molec. cell. Biol.* **10,** 6524–6532 (1990).
17. Nicholson, R. C. *et al. EMBO J.* **9,** 4443–4454 (1990).
18. Yang-Yen, H. F. *et al. Cell* **62,** 1205–1215 (1990).
19. Schule, R. *et al. Cell* **62,** 1217–1226 (1990).
20. Pfahl, M. *Endocr. Rev.* **5,** 651–658 (1993).
21. Fisher, G. J. *et al. J. biol. Chem.* **269,** 20629–20635 (1994).
22. Weinstein, G. D. & Boucek, R. J. *J. invest. Dermat.* **35,** 227–229 (1960).
23. Bailly, B. S. *et al. J. invest. Dermat.* **94,** 47–51 (1990).
24. Rafal, E. S. *et al. New. Engl. J. Med.* **326,** 368–374 (1992).
25. Hill, P. A. *et al. Biochem. J.* **308,** 167–175 (1995).
26. Fisher, G. J. *et al. J. invest. Dermat.* **96,** 699–707 (1991).
27. Hu, C. L., Crombie, G. & Franzblau, C. *Analyt. Biochem.* **88,** 638–643 (1978).
28. Hibbs, M. S., Hasty, K. A., Seyer, J. M., Kang, A. H. & Mainardi, C. L. *J. biol. Chem.* **260,** 2493–2500 (1985).
29. Werb, Z., Tremble, P. M., Behrendtsen, O., Crowley, E. & Damsky, C. H. *J. Cell Biol.* **109,** 877–889 (1989).
30. Murphy, G. *et al. Biochem. J.* **258,** 463–472 (1989).

ACKNOWLEDGEMENTS. All authors contributed equally to this work. We thank C. Peterson for help in tissue procurement; T. Hamilton for statistical analyses; J.-H. Xiao for SP-1 gel-shift assays; G. Goldberg for 92K cDNA; C. Brinkerhoff for stromelysin I cDNA; R. Breathnach for stromelysin II cDNA; G. Murphy for 92K antibody; H. Birkedal-Hansen for 72K antibody; and W. Parkinson for advice on optics. We obtained the interstitial collagenase antibody from the Developmental Studies Hybridoma Bank, maintained by the Department of Pharmacology and Molecular Sciences at Johns Hopkins University School of Medicine and the Department of Biology at the University of Iowa, under contract from the NICHD.

Normal host prion protein necessary for scrapie-induced neurotoxicity

Sebastian Brandner*, Stefan Isenmann*, Alex Raeber†, Marek Fischer†, Andreas Sailer†, Yasushi Kobayashi†, Silvia Marino*, Charles Weissmann† & Adriano Aguzzi*‡

* Institute of Neuropathology, Department of Pathology, University Hospital, CH-8091 Zürich, Switzerland
† Institute of Molecular Biology, Department I, University of Zürich, Switzerland

ACCUMULATION of the prion protein PrP^{Sc}, a pathological and protease-resistant isoform of the normal host protein PrP^{C}, is a feature of prion disease such as scrapie[1,2]. It is still unknown whether scrapie pathology comes about by neurotoxicity of PrP^{Sc}, acute depletion of PrP^{C}, or some other mechanism. Here we investigate this question by grafting neural tissue overexpressing PrP^{C} into the brain of PrP-deficient mice which are scrapie-resistant and do not propagate infectivity[3–5]. After intracerebral inoculation with scrapie prions, the grafts accumulated high levels of PrP^{Sc} and infectivity and developed the severe histopathological changes characteristic of scrapie. Moreover, substantial amounts of graft-derived PrP^{Sc} migrated into the host brain. Even 16 months after inoculation no pathological changes were seen in PrP-deficient tissue, not even in the immediate vicinity of the grafts. Therefore, in addition to being resistant to scrapie infection, brain tissue devoid of PrP^{C} is not damaged by exogenous PrP^{Sc}.

We exposed brain tissue of PrP-deficient (*Prn-p*$^{o/o}$) mice to a continuous source of PrP^{Sc} by grafting embryonic telencephalic tissue from transgenic mice overexpressing PrP into the caudoputamen or lateral ventricles of *Prn-p*$^{o/o}$ mice and inoculating it with scrapie prions. The donors, transgenic *tga20* mice[6], contain an array of 30–50 gene copies encoding PrP, overexpress PrP^{C} 5–8 fold, and show incubation times of around 60 days as compared to 160 days for CD-1 wild-type mice. In the terminal stage of scrapie both mouse strains exhibit similar prion titres whereas PrP^{Sc} levels in *tga20* are 25–50% lower than in CD-1 brain[6]. Twenty-six *Prn-p*$^{o/o}$ animals engrafted with *tga20* tissue, three with wild-type and seven with *Prn-p*$^{o/o}$ tissue, were inoculated intracerebrally with scrapie prions. All mice remained free of scrapie symptoms for at least 70 weeks; this exceeds the survival time of scrapie-infected *tga20* mice sevenfold. However, *tga20* and wild-type grafts developed characteristic histopathological features of scrapie 70 and 160 days after inoculation (p.i.), respectively, reflecting the incubation time of scrapie in the respective donor animals[4,6]. Infection of wild-type mice harbouring *tga20* grafts ($n = 4$) induced scrapie pathology in both graft and host brain, indicating efficient spread of prions from host to graft (Fig. 1*a–c*). Uninfected ($n = 9$) or mock-infected ($n = 7$) *tga20* grafts occasionally showed mild gliosis but never spongiosis (Fig. 1*d–f*). Therefore, high expression of PrP by itself did not induce neurodegeneration in grafts.

Early stages of the disease in the graft (70–140 days p.i.) were characterized by spongiosis, gliosis and reduced synaptophysin immunoreactivity (Fig. 1*g–i*), which we found in terminally sick *tga20* mice, whereas intermediate-stage grafts (140–280 days p.i.) showed *status spongiosus* with dramatic ballooning and loss of neurons, gliosis and stripping of neuronal processes (Fig. 1*j–l*). At

‡To whom correspondence should be addressed.